Multistability

International Edition: DOI: 10.1002/anie.201511281
German Edition: DOI: 10.1002/ange.201511281

Direct Observation of Ordered High-Spin–Low-Spin Intermediate States of an Iron(III) Three-Step Spin-Crossover Complex

Zhao-Yang Li[+], Hiroyoshi Ohtsu[+], Tatsuhiro Kojima, Jing-Wei Dai, Takefumi Yoshida, Brian K. Breedlove, Wei-Xiong Zhang, Hiroaki Iguchi, Osamu Sato,* Masaki Kawano, and Masahiro Yamashita**

Abstract: *A neutral mononuclear Fe^{III} complex $[Fe^{III}$(H-5-Br-thsa-Me)(5-Br-thsa-Me)]·H_2O (**1**; H_2-5-Br-thsa-Me = 5-bromosalicylaldehyde methylthiosemicarbazone) was prepared that exhibited a three-step spin-crossover (SCO) with symmetry breaking and a 14 K hysteresis loop owing to strong cooperativity. Two ordered intermediate states of **1** were observed, 4HS–2LS and 2HS–4LS, which exhibited reentrant phase-transition behavior. This study provides a new platform for examining multistability in SCO complexes.*

Spin-crossover (SCO) complexes have been among the most intensively studied switchable molecular materials over the last few decades.[1] Reversible switching between the high-spin (HS) and the low-spin (LS) states is generally accompanied by changes in various properties of the material, such as magnetic, optical, and dielectric properties, and has potential applications in information storage, sensors, and visual displays.[2] More recently, the focus of SCO research has turned towards complexes with multiple states, such as tristable and multistable systems.[3] Such systems can be used in new molecular devices, such as multiswitches and ternary memory devices.

Thus, complexes that exhibit two-step and three-step spin transitions are sought.[4] $[Fe^{II}(2\text{-pic})_3]Cl_2·C_2H_5OH$ (2-pic = 2-picolylamine) exhibits a two-step SCO phenomenon, and by using X-ray diffraction and heat-capacity measurements, it has been shown that Fe^{II} SCO sites form a long-range periodic structure with a HS/LS ratio of 1:1 in the intermediate state.[5] A few examples of mononuclear,[6] polymeric,[7] and polynuclear[4a,c,8] Fe^{II} complexes which undergo two-step spin transitions have also been reported.[9]

Oshio and co-workers have reported a rare multistep multicomponent system, $[Fe^{II}(dpp)_2][Ni(mnt)_2]_2·MeNO_2$, which undergoes low-temperature dimerization of the $[Ni(mnt)_2]$ units (dpp = 2,6-bis(pyrazol-1-yl)pyridine and mnt = maleonitriledithiolate).[10] A two-dimensional (2D) Hofmann-like network, $[Fe^{II}(4\text{-methylpyridine})_2(Au(CN)_2)]$, has been reported to undergo a three-step SCO transition, of which the structures of the intermediate states are unknown.[4h] Moreover, Kepert and co-workers have reported a three-step SCO three-dimensional pillared Hofmann-type metal–organic framework (MOF), which exhibits long-range ordering of HS and LS sites in the intermediate states studied by using synchrotron-based powder X-ray diffraction (PXRD).[4g] We have reported an example of a five/six-step SCO transition without periodic ordering in the intermediate states, during which symmetry breaking occurs.[11]

It has been recognized that the spin transition strongly depends on cooperativity, which results from local structural distortions associated with the molecular spin-state change, coupled to long-range interactions of elastic origins in the crystalline solid.[12] These interactions are primarily mediated by intermolecular contacts, such as hydrogen bonds, π–π stacking, and van der Waals interactions within the crystal lattice.[13]

Although a few multistep Fe^{II} SCO complexes have been reported, Fe^{III} complexes exhibiting multistep (above three steps) spin transitions with periodicity have not been reported. In other words, long-range ordering of HS and LS sites in the intermediate states is extremely difficult owing to the poor cooperativity among the Fe^{III} SCO complexes. Thus, we focused on enhancing the cooperativity among ferric SCO complexes by incorporating hydrogen bonding. In this study, we designed a new ligand that could act as a hydrogen-bond donor and accepter to produce an SCO complex with reversible multistability; the resulting complex underwent abrupt thermal transitions with hysteresis.

[*] Dr. Z. Y. Li,[+] Dr. J. W. Dai, T. Yoshida, Dr. B. K. Breedlove, Dr. H. Iguchi, Prof. M. Yamashita
Department of Chemistry, Graduate School of Science
Tohoku University
6-3 Aramaki-Aza-Aoba, Aoba-ku, 980-8578, Sendai (Japan)
E-mail: jingweiii@gmail.com
yamasita.m@gmail.com

Dr. H. Ohtsu,[+] Prof. M. Kawano
Division of Advanced Materials Science, Pohang University of Science and Technology (POSTECH), RIST Building 3-3390
77 Cheongam-Ro, Nam-Gu, Pohang (South Korea)

Dr. T. Kojima
Department of Chemistry, Graduate School of Science
Osaka University
Toyonaka, Osaka, 560-0043 (Japan)

Prof. O. Sato
Institute for Materials Chemistry and Engineering
Kyushu University
6-10-1 Hakozaki, Higashiku, Fukuoka, 812-8581 (Japan)
E-mail: sato@cm.kyushu-u.ac.jp

Dr. W. X. Zhang
MOE Key Laboratory of Bioinorganic and Synthetic Chemistry
School of Chemistry and Chemical Engineering
Sun Yat-Sen University
Guangzhou 510275 (P.R. China)

[+] These authors contributed equally to this work.

Supporting information for this article can be found under: http://dx.doi.org/10.1002/anie.201511281.

Herein we report a new neutral mononuclear complex, $[Fe^{III}(H\text{-}5\text{-}Br\text{-}thsa\text{-}Me)(5\text{-}Br\text{-}thsa\text{-}Me)]\cdot H_2O$ (**1**; H_2-5-Br-thsa-Me = 5-bromosalicylaldehyde methylthiosemicarbazone; see Figure S1 in the Supporting Information for the structure of the ligand), which exhibited a three-step spin transition in both cooling and heating processes (Figure 1). Thermal

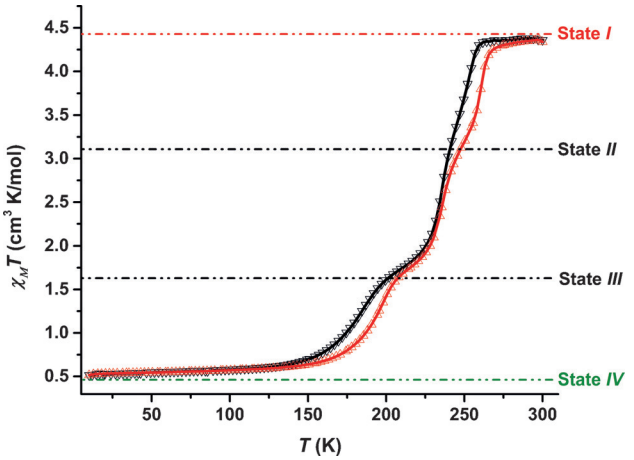

Figure 1. Temperature dependence of the magnetic susceptibility of **1** measured in the *T* range of 5–300 K in a 5000 Oe field. A complete, reversible three-step SCO was observed (red and black curves represent heating and cooling processes, respectively).

hysteresis was observed between states I and II (ca. 8 K) and between states III and IV (ca. 14 K). Remarkable long-range ordering accompanies this stepwise magnetic transition: The molecule converted from all HS states to long-range configurations of ordered intermediate states and then to all LS states (i.e. all HS→4HS–2LS→2HS–4LS→all LS), which were directly observed by using synchrotron single-crystal X-ray diffraction (SC-XRD).

Complex **1** was synthesized by heating the H_2-5-Br-thsa-Me ligand, dimethylamine, and $Fe(NO_3)_3\cdot 9H_2O$ at reflux in a mixture of methanol and water. To observe the three-step spin-transition behavior, extremely good crystals of the products were needed. PXRD at room temperature confirmed the purity and crystallinity of the complex (see Figure S2).

Magnetic susceptibility measurements were performed on single crystals in the temperature (*T*) range of 5–300 K during both heating and cooling processes. The $\chi_M T$ value at 300 K was estimated to be 4.18 $cm^3 K mol^{-1}$, which is close to the expected value of 4.375 $cm^3 K mol^{-1}$ for HS Fe^{III} ions ($S = 5/2$). On further cooling, a stepwise decrease in the $\chi_M T$ value occurred from 4.18 to 0.54 $cm^3 K mol^{-1}$ while cooling from 300 to 5 K, thus indicating that a spin transition from the HS to the LS state occurred. The first transition step in the cooling mode was centered at $T1\downarrow = 253$ K, and the $\chi_M T$ value decreased to approximately 3.19 $cm^3 K mol^{-1}$ at 245 K, which indicated a spin-state conversion involving about 30% of the LS Fe^{III} centers. The second transition step was centered at 236 K (T2↓), and the $\chi_M T$ value decreased abruptly to a value of approximately 1.67 $cm^3 K mol^{-1}$ at 205 K, thus indicating that a spin-state conversion occurred involving about 70% of the LS Fe^{III} centers. Further cooling gradually led to a third transition step centered at 189 K (T3↓), which indicated complete conversion of the Fe^{III} centers. On the other hand, in the heating mode, the three transition steps were centered at 202 (T1↑), 236 (T2↑), and 260 K (T3↑) with a hysteresis of approximately 14 K between states III and IV, approximately 2 K between II and III, and approximately 8 K between I and II with a scan rate of 5 $K min^{-1}$.

Next, we investigated the effects of the scan rate on the hysteresis (see Figure S3). At all scan rates, the three-step hysteresis was observed during the cooling and heating processes (see Table S1 in the Supporting Information). However, only the loop width was slightly dependent on the scan rate; the shape of the loop was not affected. The largest ΔT values were 14 K between states III and IV at 5 $K min^{-1}$ and 10 K between states I and II at 8 $K min^{-1}$, mainly because the barrier for spin conversion between the HS and LS states is not large. The results indicate that **1** undergoes a complete three-step spin transition via two intermediate states: state I (HS)↔state II (2:1 HS/LS)↔state III (1:2 HS/LS)↔state IV (LS). To the best of our knowledge, no mononuclear Fe^{III} complex exhibiting multistep hysteresis, that is, multistability, has been reported previously.

We performed differential scanning calorimetry (DSC) measurements to confirm the above results (see Figure S4). We observed a sharp peak at approximately 260 K and two smaller peaks at 200 and 238 K, respectively, in the heating mode, whereas three peaks at approximately 194, 235, and 254 K were observed in the cooling mode, thus confirming the presence of the hysteresis loop. These results support the occurrence of a cooperative first-order transition.

Next, we studied the metastable state of **1** (state V). When the sample was irradiated with 532 nm continuous-wave laser light at 5 K, an increase in magnetization was observed (see Figure S5), thus indicating that light-induced excited-spin-state trapping (LIESST) occurred. The $\chi_M T$ value increased from an initial value of 0.54 $cm^3 K mol^{-1}$ to a saturation regime at 0.90 $cm^3 K mol^{-1}$ over 2 h, and then upon heating, the metastable state relaxed back to the LS state at approximately 70 K, thus indicating that approximately 10% photoconversion from the LS to a metastable HS state (state V) occurred. It is known that approximately 10% photoconversion is normal for ferric complexes owing to the relatively fast relaxation of the photoinduced HS state, and only the Fe^{III} species in the surface layer exhibit the LIESST effect because Fe^{III} complexes strongly absorb in the visible region. In general, one-step thermal relaxation of the metastable state (state V) is common because the metastable state is not completely the same as the HS state. This result clearly suggests that **1** is a photoresponsive complex.

SC-XRD was performed on the same single crystal at various *T* values in the synchrotron beamline NW2A at KEK, Japan. In the first stage, oscillation photographs were acquired along the c^* axis of the crystal to verify the differences in the Bragg reflections for states I–IV at 295, 245, 205, and 100 K, respectively. The *c* axis parameter tripled on the basis of the extra Bragg reflections (Figure 2), thus

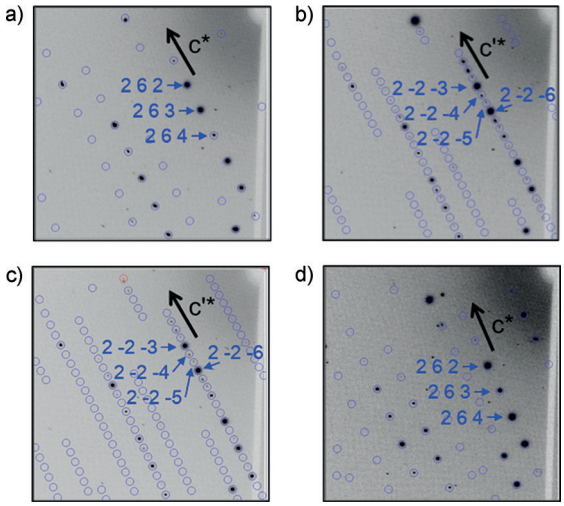

Figure 2. Single-crystal diffraction images along the *c** direction at a) 100 K and d) 295 K; and along the *c'** direction at b) 205 K and c) 245 K. New Bragg reflections appeared in images of the intermediate states. The *c** direction was determined from indices derived from the data obtained at 100 and 295 K, and the *c'** direction was determined from indices derived from the data obtained at 205 and 245 K.

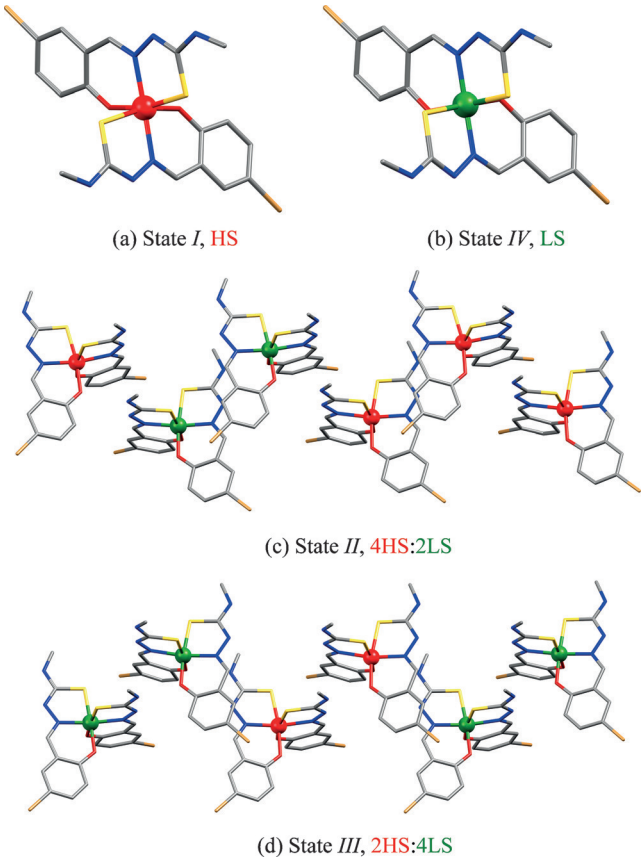

Figure 3. Crystal structures for the different states of complex **1** with H atoms omitted for clarity: a) state I, all HS; b) state IV, all LS; c) state II, 4HS–2LS; d) state III, 2HS–4LS.

clearly indicating the ordering of the spin states in the intermediate states (states II and III).

Moreover, we were able to fully characterize the single-crystal structure of each state, including intermediate states II and III (see Table S2 for a summary of crystal data). At 295 K (state I, HS), complex **1** was determined to be in the monoclinic *Cc* space group (Flack parameter: 0.005(3)): $a=8.9090(1)$, $b=23.1573(2)$, $c=11.4302(1)$ Å, and $V=2357.63(4)$ Å^3. The asymmetric unit consists of one independent Fe^{III} center, H-5-Br-thsa and 5-Br-thsa ligands, and an uncoordinated water molecule (Figure 3a). The metal center is hexacoordinate with an $N_2O_2S_2$ donor set. The Fe–N and Fe–S bond distances at 295 K were determined to be 2.113(4)/2.135(4) and 2.394(2)/2.450(2) Å, respectively, which are characteristic of HS Fe^{III} complexes.

When *T* was decreased from room temperature to 245 K (state II), the crystal quality did not decrease, and the crystal data indicated that the symmetry was reduced to the triclinic *P*1 space group (Flack parameter: 0.017 (4)) with six crystallographically distinct Fe^{III} molecules: $a=8.9133(1)$, $b=12.4010(1)$, $c=34.0378(4)$ Å, and $V=3510.33(7)$ Å^3. As compared to state I, the *a* axis of state II is barely changed. However, the *b* and c axes are nearly half and three times as long than those of state I (see Figure S6), consistent with the results of the SC oscillation photograph studies.

For state II, each molecule has the same coordination environment with an $N_2O_2S_2$ donor set but a different geometry (Figure 3c). From the average bond lengths (Fe1–N: 2.011(6) Å, Fe2–N: 2.018(6) Å), Fe1 and Fe2 are mainly LS ions, whereas Fe3, Fe4, Fe5, and Fe6 molecules are mainly HS ions (Table 1). This result clearly indicates that HS and LS

Table 1: Fe–N and Fe–S bond lengths [Å] of complex **1** at 100, 205, 245, and 295 K.

T	100 K	205 K	245 K	295 K
Fe1–N	1.946(2)/1.952(2)	1.966(6)/1.985(5)	2.000(6)/2.022(6)	2.113(4)/2.135(4)
Fe2–N	–	1.996(6)/2.019(5)	2.017(6)/2.020(6)	–
Fe3–N	–	2.011(7)/2.016(6)	2.080(6)/2.103(6)	–
Fe4–N	–	1.966(7)/1.983(6)	2.047(6)/2.053(6)	–
Fe5–N	–	2.037(6)/2.063(6)	2.088(6)/2.095(6)	–
Fe6–N	–	2.035(7)/2.059(6)	2.049(6)/2.059(6)	–
Fe_{LS}–N[a]	1.949(2)	1.993(6)	2.015(6)	–
Fe_{HS}–N[a]	–	2.049(6)	2.072(6)	2.124(4)
Fe1–S	2.243(1)/2.261(1)	2.255(2)/2.286(2)	2.292(2)/2.332(3)	2.394(2)/2.450(2)
Fe2–S	–	2.285(3)/2.321(2)	2.297(3)/2.333(3)	–
Fe3–S	–	2.299(3)/2.330(4)	2.372(4)/2.417(3)	–
Fe4–S	–	2.261(3)/2.288(2)	2.323(4)2.369(4)	–
Fe5–S	–	2.333(3)/2.369(4)	2.370(3)/2.417(4)	–
Fe6–S	–	2.334(4)/2.371(3)	2.338(4)/2.372(5)	–
Fe_{LS}–S[b]	2.252(1)	2.291(3)	2.314(3)	–
Fe_{HS}–S[b]	–	2.352(3)	2.372(4)	2.422(2)

[a] Average Fe–N bond length. [b] Average Fe–S bond length.

states of the Fe^{III} sites are ordered in state II in a HS/LS ratio of 4:2 (4HS:2LS), which is consistent with the analysis of the magnetic data ($\chi_M T = 3.2\ cm^3\,K\,mol^{-1}$, ca. 70% HS states).

At 205 K (Figure 3d, state III), new Bragg reflections appeared in the oscillation photographs along the c'^* axis. The diffraction data indicate that there are six crystallographically independent Fe^{III} molecules, of which Fe1, Fe2, Fe3, and Fe4 are mainly LS and Fe5 and Fe6 are HS. As for state II, the triclinic $P\bar{1}$ space group was observed (Flack parameter: 0.006(3)): $a = 8.9127(1)$, $b = 12.3885(1)$, $c = 33.894(4)$ Å, and $V = 3491.76(7)$ Å^3. The data clearly show that the ratio of HS and LS sites is 2:4, which is consistent with the magnetic data ($\chi_M T = 1.5\ cm^3\,K\,mol^{-1}$, ca. 30% HS states).

At 100 K (Figure 3b, state IV), the symmetry changed to the monoclinic *Cc* space group (Flack parameter: 0.015(2)), thus indicating that the unit cell contains only one LS Fe^{III} complex: $a = 8.9000(1)$, $b = 23.0478(2)$, $c = 11.2492(1)$ Å, and $V = 2306.87(4)$ Å^3. The extra Bragg reflections disappeared at 100 K (Figure 2a), thus indicating that the 2HS–4LS ordered state disappeared and the state IV formed. The Fe–N and Fe–S bond distances were 1.946(2)/1.952(2) and 2.243(1)/2.261-(1) Å at 100 K, respectively, which correspond to an LS Fe^{III} center.

The one-dimensional (1D) packing structure of **1** in states I and IV is similar, with ordered regions of molecules of the same spin states (Figure 4). However, in the packing structures of the intermediate states, there are ordered regions of HS and LS sites. For state II, long-range ordering of [4HS–2LS] moieties was observed, whereas for state III, long-range ordering of [2HS–4LS] units was observed. The ordering of the HS and LS sites in the packing structure is mediated by two sets of intermolecular hydrogen-bonding interactions. There are three kinds of hydrogen bonding (see Figure S7). One is intermolecular hydrogen bonding with water molecules (i.e., $O_{(water)}$–H···$O_{(C–O)}$), which are present in each state. The second is intermolecular hydrogen bonding between the molecules of **1** (i.e., $N_{(amide)}$–H···$O_{(C–O)}$). These H bonds are relatively strong noncovalent interactions in the LS state (donor–acceptor (D···A) distances are 2.713(4)/2.826(4) Å, D-H-A angles are 167/175°), whereas they are somewhat weaker in the HS states (D···A distances are 2.822(6)/2.929(6) Å, D-H-A angles are 168°/174°). Thus, the HS state is arranged in a zigzag chain structure. The last type of intermolecular hydrogen bonding is that with H_2O molecules bridging molecules of **1** (i.e., $N_{(azomethine)}$–H···$O_{(water)}$ and $O_{(water)}$–H···$N_{(azomethine)}$) and causes the formation of a 1D chain structure. A mixture of the last two types of H bonding significantly contributes to the 2D structure and the ordering of the HS and LS sites (Figure 5), as well as the spin transitions and structural variations.

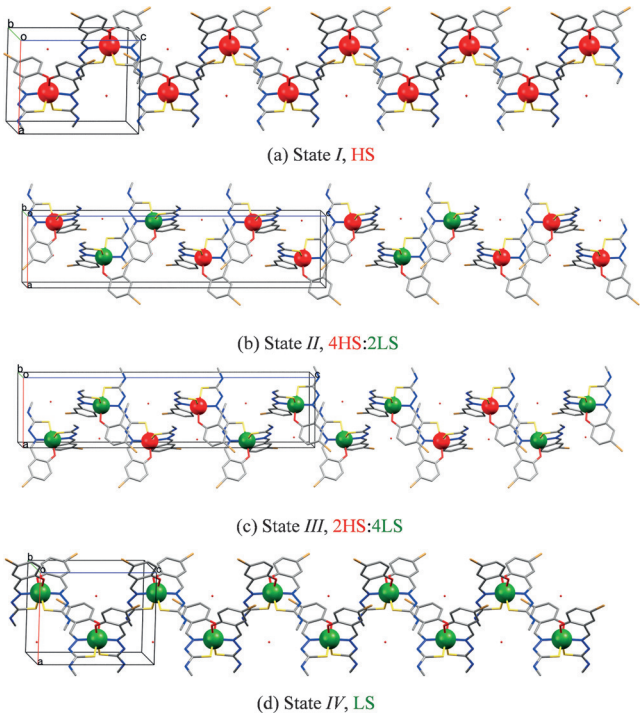

Figure 4. Packing structures of the four different states of **1**: a) state I; b) state II; c) state III; d) state IV. The ordering of HS (red) and LS molecules (green) is clear.

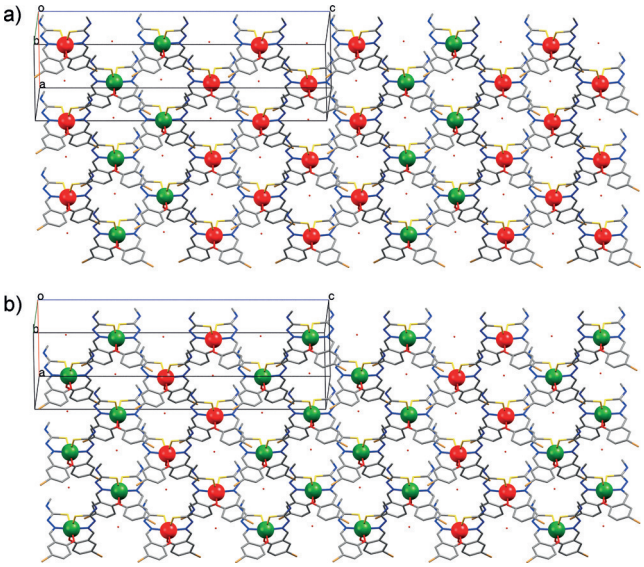

Figure 5. 2D packing structures of the intermediate states with different distributions of HS and LS sites: a) state II; b) state III.

To gain a deeper understanding of the mechanism for the three-step spin transition in neutral Fe^{III} mononuclear complexes with strong cooperativity, we compared several models that may be applied to the present case. The Ising-type HS/LS models derived from the Gorski–Bragg–Williams or Slichter–Drickamer approach assume a single crystallographic Fe site in a mean environment (mean field) and neglects correlation effects.[14] However, Landau theory, which explicitly accounts for changes in crystal symmetry and the coupling of the ordering and spin-transition processes, is applicable for the present three-step spin transition because long-range elastic interactions depend upon strong intermolecular contacts to communicate the spin transition to every Fe^{III} center in the lattice. DFT calculations and simulations based on a modified Landau theory are currently in progress to elucidate the

crystallographic symmetry breaking accompanying the multistep spin-transition behavior of **1**.

In summary, we have prepared the first neutral mononuclear multistep Fe^{III} SCO complex, which underwent symmetry breaking and exhibits a 14 K hysteresis loop. X-ray diffraction analysis clearly indicated that there were four spin states (states I–IV) with different long-range orderings of the HS and LS sites and one metastable spin state (state V). Two ordered intermediate states of **1** were observed: 4HS–2LS (state II) and 2HS–4LS (state III), which exhibit reentrant phase-transition behavior. Furthermore, this study provides a new platform for examining multistability in SCO complexes because it is possible to control the number of stable states by increasing the flexibility to allow for symmetry breaking and to incorporate hydrogen bonds to enhance cooperativity.

Experimental Section

The Schiff base ligand H_2-5-Br-thsa-Me (H_2L) was synthesized by a condensation reaction of 2-hydroxy-5-bromobenzaldehyde and 4-methylthiosemicarbazide. The product was purified in hot ethanol and obtained in 70% yield. Single crystals suitable for X-ray crystallographic analysis (see the Supporting Information) were obtained by recrystallization from ethanol. Elemental analysis (%) calcd for $C_9H_{10}BrN_3OS$: H 3.50, C 37.51, N 14.58; found: H 3.47, C 37.62, N 14.43.

Synthesis of $[Fe^{III}(H\text{-}5\text{-}Br\text{-}thsa\text{-}Me)(5\text{-}Br\text{-}thsa\text{-}Me)]\cdot H_2O$ (**1**): H_2-5-Br-thsa-Me (0.288 g, 1 mmol) and a solution of 45% DMA (0.225 g, 2 mmol) in methanol were heated in methanol (50 mL) and water (0.5 mL) at 80 °C. $Fe(NO_3)_3\cdot 9H_2O$ (0.202 g, 0.5 mmol) was slowly added, and the resulting mixture was heated at reflux for a further 8 h and then allowed to cool to room temperature overnight. The black precipitate that formed was collected by filtration, washed with acetone/water, and dried in a vacuum for 4 h. Single crystals suitable for X-ray diffraction were obtained through a layering reaction in about 55% yield. Elemental analysis (%) calcd for $C_{18}H_{19}Br_2FeN_6O_3S_2$: H 2.96, C 33.41, N 12.99; found: H 2.93, C 33.77, N 12.76.

Acknowledgements

Z.Y.L. is grateful for financial support from the Japan Society for the Promotion of Science (JSPS). The X-ray diffraction study with synchrotron radiation was performed at the PF-AR (NW2A Beamline) of the High Energy Accelerator Research Organization (KEK; proposal no. 2014G008) and at the Pohang Accelerator Laboratory (Beamline 2D) supported by POSTECH.

Keywords: cooperativity · iron · multistability · spin crossover · symmetry breaking

How to cite: *Angew. Chem. Int. Ed.* **2016**, *55*, 5184–5189
Angew. Chem. **2016**, *128*, 5270–5275

[1] a) P. Gütlich, H. A. Goodwin, *Top. Curr. Chem.* **2004**, *233*, 1–47; b) P. Gütlich, Y. Garcia, H. A. Goodwin, *Chem. Soc. Rev.* **2000**, *29*, 419–427; c) E. Breuning, M. Ruben, J. M. Lehn, F. Renz, Y. Garcia, V. Ksenofontov, P. Gütlich, E. Wegelius, K. Rissanen, *Angew. Chem. Int. Ed.* **2000**, *39*, 2504–2507; *Angew. Chem.* **2000**, *112*, 2563–2566.

[2] a) J. F. Létard, P. Guionneau, L. Goux-Capes, *Top. Curr. Chem.* **2004**, *235*, 221–249; b) Y. S. Koo, J. R. Galan-Mascaros, *Adv. Mater.* **2014**, *26*, 6785–6789; c) J. Linares, E. Codjovi, Y. Garcia, *Sensors* **2012**, *12*, 4479–4492.

[3] a) A. B. Gaspar, V. Ksenofontov, M. Seredyuk, P. Gütlich, *Coord. Chem. Rev.* **2005**, *249*, 2661–2676; b) J. A. Real, A. B. Gaspar, M. C. Muñoz, *Dalton Trans.* **2005**, 2062–2079.

[4] a) M. Nihei, M. Ui, M. Yokota, L. Q. Han, A. Maeda, H. Kishida, H. Okamoto, H. Oshio, *Angew. Chem. Int. Ed.* **2005**, *44*, 6484–6487; *Angew. Chem.* **2005**, *117*, 6642–6645; b) A. J. Simaan, M.-L. Boillot, E. Rivière, A. Boussac, J.-J. Girerd, *Angew. Chem. Int. Ed.* **2000**, *39*, 196–198; *Angew. Chem.* **2000**, *112*, 202–204; c) R. J. Wei, Q. Huo, J. Tao, R. B. Huang, L. S. Zheng, *Angew. Chem. Int. Ed.* **2011**, *50*, 8940–8943; *Angew. Chem.* **2011**, *123*, 9102–9105; d) A. Bousseksou, G. Molnar, J. A. Real, K. Tanaka, *Coord. Chem. Rev.* **2007**, *251*, 1822–1833; e) Z. Y. Li, J. W. Dai, K. J. Gagnon, H. L. Cai, T. Yamamoto, Y. Einaga, H. H. Zhao, S. Kanegawa, O. Sato, K. R. Dunbar, R. G. Xiong, *Dalton Trans.* **2013**, *42*, 14685–14688; f) S. Zein, S. A. Borshch, *J. Am. Chem. Soc.* **2005**, *127*, 16197–16201; g) N. F. Sciortino, K. R. Scherl-Gruenwald, G. Chastanet, G. J. Halder, K. W. Chapman, J.-F. Létard, C. J. Kepert, *Angew. Chem. Int. Ed.* **2012**, *51*, 10154–10158; *Angew. Chem.* **2012**, *124*, 10301–10305; h) T. Kosone, I. Tomori, C. Kanadani, T. Saito, T. Mochida, T. Kitazawa, *Dalton Trans.* **2010**, *39*, 1719–1721.

[5] a) L. Wiehl, G. Kiel, C. P. Köhler, H. Spiering, P. Gütlich, *Inorg. Chem.* **1986**, *25*, 1565–1571; b) R. Jakobi, H. Spiering, P. Gütlich, *J. Phys. Chem. Solids* **1992**, *53*, 267–275; c) P. Gütlich, A. Hauser, H. Spiering, *Angew. Chem. Int. Ed. Engl.* **1994**, *33*, 2024–2054; *Angew. Chem.* **1994**, *106*, 2109–2141; d) H. Romstedt, A. Hauser, H. Spiering, *J. Phys. Chem. Solids* **1998**, *59*, 265–275; e) D. Chernyshov, M. Hostettler, K. W. Törnroos, H.-B. Bürgi, *Angew. Chem. Int. Ed.* **2003**, *42*, 3825–3830; *Angew. Chem.* **2003**, *115*, 3955–3960; f) M. Hostettler, K. W. Törnroos, D. Chernyshov, B. Vangdal, H.-B. Bürgi, *Angew. Chem. Int. Ed.* **2004**, *43*, 4589–4594; *Angew. Chem.* **2004**, *116*, 4689–4695; g) K. W. Törnroos, M. Hostettler, D. Chernyshov, B. Vangdal, H.-B. Bürgi, *Chem. Eur. J.* **2006**, *12*, 6207–6215.

[6] a) B. J. C. Vieira, J. T. Coutinho, I. C. Santos, L. C. J. Pereira, J. C. Waerenborgh, V. da Gama, *Inorg. Chem.* **2013**, *52*, 3845–3850; b) J. PowerLuan, J. Zhou, Z. Liu, B. W. Zhu, H. S. Wang, X. Bao, W. Liu, M. L. Tong, G. Peng, H. N. Peng, L. Salmon, A. Bousseksou, *Inorg. Chem.* **2015**, *54*, 5145–5147; c) Q. Yang, X. Cheng, Y. X. Wang, B. W. Wang, Z. M. Wang, S. Gao, *Dalton Trans.* **2015**, *44*, 8938–8941; d) T. Sato, K. Nishi, S. Iijima, M. Kojima, N. Matsumoto, *Inorg. Chem.* **2009**, *48*, 7211–7229; e) J. Klingele, D. Kaase, M. H. Klingele, J. Lach, S. Demeshko, *Dalton Trans.* **2010**, *39*, 1689–1691; f) S. Bonnet, M. A. Siegler, J. S. Costa, G. Molnar, A. Bousseksou, A. L. Spek, P. Gamez, J. Reedijk, *Chem. Commun.* **2008**, 5619–5621; g) S. Bonnet, G. Molnar, J. S. Costa, M. A. Siegler, A. L. Spek, A. Bousseksou, W. T. Fu, P. Gamez, J. Reedijk, *Chem. Mater.* **2009**, *21*, 1123–1136.

[7] a) M. M. Dîrtu, F. Schmit, A. D. Naik, I. Rusu, A. Rotaru, S. Rackwitz, J. A. Wolny, V. Schunemann, L. Spinu, Y. Garcia, *Chem. Eur. J.* **2015**, *21*, 5843–5855; b) T. Delgado, A. Tissot, C. Besnard, L. Guénée, P. Pattison, A. Hauser, *Chem. Eur. J.* **2015**, *21*, 3664–3670; c) T. Romero-Morcillo, F. J. Valverde-Muñoz, M. C. Muñoz, J. M. Herrera, E. Colacio, J. A. Real, *RSC Adv.* **2015**, *5*, 69782–69789; d) G. J. Halder, K. W. Chapman, S. M. Neville, B. Moubaraki, K. S. Murray, J. F. Letard, C. J. Kepert, *J. Am. Chem. Soc.* **2008**, *130*, 17552–17562; e) J. A. Rodríguez-Velamazán, C. Carbonera, M. Castro, E. Palacios, T. Kitazawa, J.-F. Létard, R. Burriel, *Chem. Eur. J.* **2010**, *16*, 8785–8796; f) S. M. Neville, B. A. Leita, G. J. Halder, C. J. Kepert, B.

Moubaraki, J.-F. Létard, K. S. Murray, *Chem. Eur. J.* **2008**, *14*, 10123 – 10133; g) V. Martínez, A. B. Gaspar, M. C. Muñoz, G. V. Bukin, G. Levchenko, J. A. Real, *Chem. Eur. J.* **2009**, *15*, 10960 – 10971.

[8] a) J. A. Real, A. B. Gaspar, M. C. Muñoz, P. Gütlich, V. Ksenofontov, H. Spiering, *Top. Curr. Chem.* **2004**, *233*, 167 – 193; b) J. A. Real, H. Bolvin, A. Bousseksou, A. Dworkin, O. Kahn, F. Varret, J. Zarembowitch, *J. Am. Chem. Soc.* **1992**, *114*, 4650 – 4658; c) V. Ksenofontov, A. B. Gaspar, V. Niel, S. Reiman, J. A. Real, P. Gütlich, *Chem. Eur. J.* **2004**, *10*, 1291 – 1298; d) J. L. M. Amoore, C. J. Kepert, J. D. Cashion, B. Moubaraki, S. M. Neville, K. S. Murray, *Chem. Eur. J.* **2006**, *12*, 8220 – 8227; e) K. Nakano, S. Kawata, K. Yoneda, A. Fuyuhiro, T. Yagi, S. Nasu, S. Morimoto, S. Kaizaki, *Chem. Commun.* **2004**, 2892 – 2893.

[9] a) M. Shatruk, H. Phan, B. A. Chrisostomo, A. Suleimenova, *Coord. Chem. Rev.* **2015**, *289*, 62 – 73; b) K. Bhar, S. Khan, J. S. Costa, J. Ribas, O. Roubeau, P. Mitra, B. K. Ghosh, *Angew. Chem. Int. Ed.* **2012**, *51*, 2142 – 2145; *Angew. Chem.* **2012**, *124*, 2184 – 2187.

[10] M. Nihei, H. Tahira, N. Takahashi, Y. Otake, Y. Yamamura, K. Saito, H. Oshio, *J. Am. Chem. Soc.* **2010**, *132*, 3553 – 3560.

[11] Z. Y. Li, J. W. Dai, Y. Shiota, K. Yoshizawa, S. Kanegawa, O. Sato, *Chem. Eur. J.* **2013**, *19*, 12948 – 12952.

[12] K. S. Murray, C. J. Kepert, *Top. Curr. Chem.* **2004**, *233*, 195 – 228.

[13] a) R. Boca, M. Boca, L. Dlhan, K. Falk, H. Fuess, W. Haase, R. Jarosciak, B. Papankova, F. Renz, M. Vrbova, R. Werner, *Inorg. Chem.* **2001**, *40*, 3025 – 3033; b) N. Nassirinia, S. Amani, S. J. Teat, O. Roubeau, P. Gamez, *Chem. Commun.* **2014**, *50*, 1003 – 1005; c) J. Y. Li, Y. C. Chen, Z. M. Zhang, W. Liu, Z. P. Ni, M. L. Tong, *Chem. Eur. J.* **2015**, *21*, 1645 – 1651; d) S. Hayami, Z. Z. Gu, H. Yoshiki, A. Fujishima, O. Sato, *J. Am. Chem. Soc.* **2001**, *123*, 11644 – 11650; e) S. M. Neville, G. J. Halder, K. W. Chapman, M. B. Duriska, B. Moubaraki, K. S. Murray, C. J. Kepert, *J. Am. Chem. Soc.* **2009**, *131*, 12106 – 12108; f) M. Nishino, K. Boukheddaden, Y. Konishi, S. Miyashita, *Phys. Rev. Lett.* **2007**, *98*, 247203; g) M. C. Young, E. Liew, J. Ashby, K. E. McCoy, R. J. Hooley, *Chem. Commun.* **2013**, *49*, 6331 – 6333; h) D. Sahoo, M. G. Quesne, S. P. de Visser, S. P. Rath, *Angew. Chem. Int. Ed.* **2015**, *54*, 4796 – 4800; *Angew. Chem.* **2015**, *127*, 4878 – 4882; i) O. Sato, *Acc. Chem. Res.* **2003**, *36*, 692 – 700.

[14] a) D. Chiruta, J. Linares, Y. Garcia, M. Dimian, P. R. Dahoo, *Physica B* **2014**, *434*, 134 – 138; b) A. Bousseksou, J. Nasser, J. Linares, K. Boukheddaden, F. Varret, *J. Phys. I* **1992**, *2*, 1381 – 1403; c) A. Bousseksou, F. Varret, J. Nasser, *J. Phys. I* **1993**, *3*, 1463 – 1473; d) C. P. Slichter, H. G. Drickamer, *J. Chem. Phys.* **1972**, *56*, 2142 – 2160; e) R. Boca, W. Linert, *Monatsh. Chem.* **2003**, *134*, 199 – 216.

Received: December 29, 2015
Published online: March 17, 2016

